Detecting separation pre-cursors using on-board optical tracking of flexible pillar sensors

O. Selim[1,*], C. Bruecker[1]

1: Dept. of Mechanical Engineering and Aeronautics, City, University of London, United Kingdom
*Corresponding author: omar.selim@city.ac.uk

Keywords: Aerodynamic separation, Bio-inspired sensor.

ABSTRACT

A novel approach for characterising specific flow phenomena unique to incipient stall in real-time on small scale UAVs and aerodynamic systems operating at low to medium Reynolds numbers is introduced. Flexible pillar sensors emanating from the suction side of an aerofoil of length approx. 3% of chord length are installed on a NACA0012 and tested at City, University of London's wind-tunnel facilities. The sensors are tracked in real-time using a high-speed camera in a simulated 'on-board' position, acting as 'digital tufts', and the results subsequently processed. The results show the pillars reacting to specific flow phenomena that are unique to incipient stall, and scale with angle of incidence. Namely, these are low-frequency oscillations of local streamwise velocity components which are hypothesised to be resulting from quasi-periodic vortex shedding/shear layer flapping from the breathing of the laminar separation bubble over the suction side.

1. Introduction

With the introduction of small and medium UAV's into every day commercial and non-commercial operations, the effects of flow separation and subsequent loss of lift at low to mid-range Reynold's numbers are becoming more and more impactful. At best, these effects can reduce the power-efficiency of an aircraft, shifting the flight out of the optimal angles of incidence, which requires consistent, drag-costly alterations of flight attitude to return to optimal flight, and at worst these effects can result in eventual catastrophic failure and loss of the system entirely. Thus, the early detection of flow separation by monitoring the pre-cursory signals is becoming ever-more important to ensure safe and efficient operation of these systems. To address this, a new concept of bio-inspired flexible pillar sensors has been developed that emanate from the suction side of the aerofoil (Fig. 1). The tips of these are tracked by a particle tracking camera placed in a simulated "on-board" position along the span of the wing section. By tracking the positions of the tips, which correlates directly to the velocities and flow structures over the aerofoil, specific phenomena unique to the critical angles of attack leading up to separated flow can be detected, thus acting as

'digital tufts' providing real-time velocity information at high temporal resolution. In practice, this would allow fail-safe, redundant, early warning of incipient flow separation to the system, allowing real-time action to be taken for aversion, or can be used for in-situ performance monitoring to give designers and engineers ample data for system performance enhancement in real-world applications in addition to experimental environments.

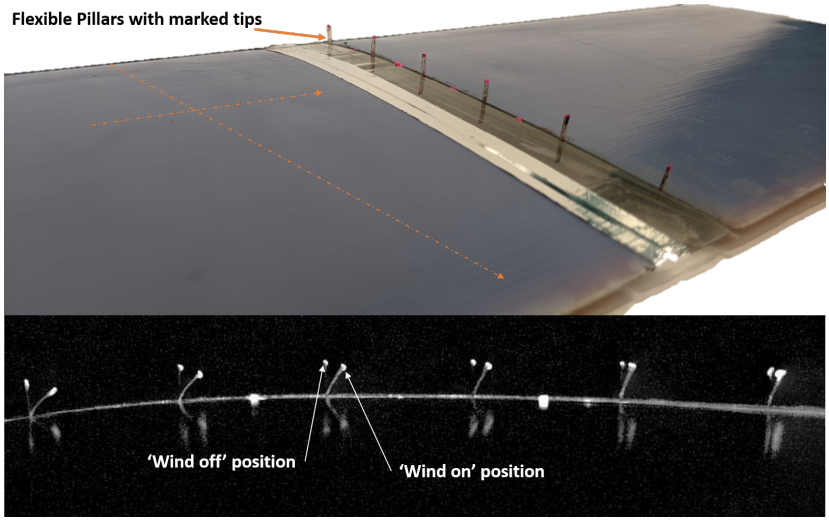

Figure 1. Top: Image from 'wing-root' position showing the different components of the model; in blue are the 3D printed aerofoil sections, and between is a transparent Perspex section, also showing the flexible pillars emanating from the surface, which could be extended to a full 'skin' with 2D arrays of sensors. Bottom: Overlain images from the tracking camera in the simulated 'on-board' position showing sample pillar deflections. (flow is left to right)

Work by (Soulier et al., 2021) has shown how in-situ optical tracking of tufts can give real-time indications of flow conditions over the surface of a wind-turbine in operation. These low-resolution techniques have already shown promising potential in optimising the efficiency of power production. Higher spatial and temporal resolution monitoring of flexible pillar structures can offer an insight into the flow structures leading up to these conditions, providing local span-wise information of those structures and phenomena incipient to separation. Such relatively subtle flow characteristics can then be detected using smaller scale sensing devices. Particularly, bio-inspired hair receptors were explored (Dickinson, 2010) for detecting changes in the boundary layer velocity profiles giving detailed information of the overall flow conditions.

Studies have shown that some quasi-periodic low frequency oscillations occur as a result of regular breathing of the Laminar Separation Bubble (LSB) formed over the suction side of an aerofoil. A study by (Winslow et al., 2018) shows the positioning of this bubble at low Reynolds number flow moving forward as angle of attack increases and settling near the suction peak location between 6 and 8 degrees. The effects of the shedding from the laminar separation bubble were observed numerically and experimentally as low-frequency oscillations in lift and drag (ElAwad & ElJack, 2019), in addition to measurements of time-resolved PIV over a NACA0012 (Tanaka, 2004). It is the aim of this phase of the research project to explore the development of a concept for an on-board optical based monitoring system that can characterise such phenomena.

The detection and response to temporal changes in flow of varying frequency ranges is nothing new to natural fliers. (Mohamed et al., 2014) have, in their investigation of biological inspired sensors in flight, discussed a variety of natural fliers using wing receptors to detect temporal flow and pressure changes, in addition to variations of amplitude for signals of the same frequency, for executive decision making in flight control and stabilisation. Even in high-speed flight, (Brücker et al., 2016) showed the ability of mechanoreceptors on fast-fliers to scale with flow conditions with a high level of sensitivity, which is critical at during high-speed stoops as small changes to angle of attack can have significant effects on lift generation and flight stability (Selim et al., 2021) .

Thus, the project aims to use optical tracking of flexible, biologically inspired pillar sensors to capture patterns correlating to flow phenomena unique to those angles of attack which are incipient to flow separation. This will offer the capability of real-time flow monitoring and provide data for flow control systems. The low frequency oscillations are captured coherently over several pillar sensor positions relatively well as opposed to how other methods may show such as, for instance, a single pressure sensor or a system of tufts. This leads into the development of a system of biologically inspired sensors which react in a predictable manner to changes in flow conditions within the flight regime of small to medium sized UAVs, which can be used in-situ to promptly provide diagnostic data to a flight control system, or can be used for diagnostics in experimental conditions.

2. Experimental Arrangement

The design and manufacturing of the pillars were based on earlier work (Li et al., 2021) using flexible micro-pillars to detect and characterise wall shear stress in the aortic artery. These were scaled up to match the scales and application of the current investigation to act as 'digital tufts' over the wing surface.

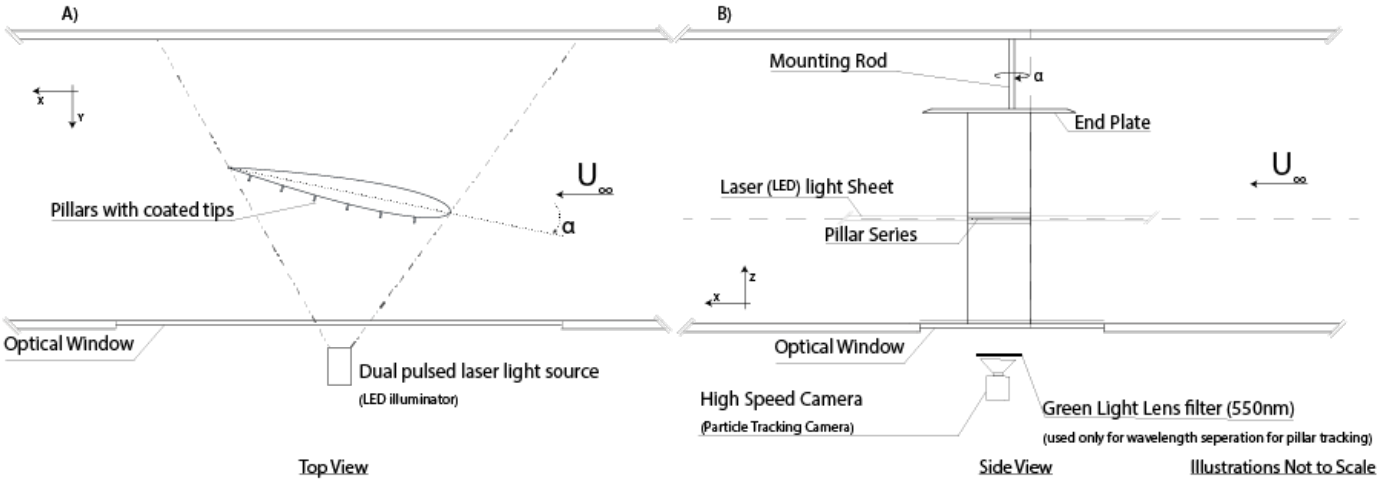

Figure 2. The experimental arrangement was such that the LED and Laser illumination were interchangeable with minimal disruption. Text between brackets indicates the alternative arrangement for the different experiments.

The model used is a 3D printed NACA-0012 section printed in two parts, with a Perspex centre section to provide optical access through the mid-span location (Fig. 1). These sections are clamped together with the sheet of pillars placed in-between. The pillars are laser cut to shape from a silicone rubber sheet, such that the sheet is clamped between the 3D printed section and the perspex section (Fig. 1). The pillar tips and specific marker points along the chord are labelled with florescent die (MMA-RhB-Frak-Paticles, Dantec Dynamics, peak emission at 584 nm, peak absorption at 540 nm) and illuminated with an LED illuminator. Thus, using optical lens filters as wavelength separation of the immitted light, the tips can be isolated from the surrounding background. A high-speed camera (ProcImage 500-Eagle high-speed camera, 1280 px × 1024 px, Photon Lines Ltd, Bloxham, UK) is mounted outside the tunnel along the span-wise line of the wing, to simulate where an on-board camera would be mounted, and fitted with a green light lens filter, thus only displaying the emission from the pillar tips and marker points. From this position the camera captures the pillar tip positions at a sampling rate of 250 Hz in two different modes; standard mode, seen in (Fig. 1) fitted with a 50mm lens, and binary mode with centroid detection of white connected pixels at a selected area in the frame, which outputs 8 time series of coordinate points corresponding to 6 pillar tips and 2 marker points. Using a 100mm lens a finer resolution can be obtained over 3 pillars of interest to allow more spatial resolution recordings. This method of data acquisition was also used to acquire position data for underwater artificial seal whiskers (Elshalakani et al., 2020). Additionally, using a Phantom M310, the same recordings were captured and the positions of those tips are then found using a MATLAB based cross-correlation code. This serves the purpose of validating the results from the tracking, and as a proof of concept for further work assembling pillars with an on-board cameras in-situ on an airborne UAV. The positions of the pillar tips were referenced with time-resolved 2D PIV carried out over the same model at a chord-wise Reynolds number of 150k for experimental validation. The experimental setup for the PIV system can be seen in (Fig. 2). A Phantom M310 camera was arranged orthogonally to the laser sheet and fitted with 100mm lens. A Litron LDY300 dual-head laser was used to illuminate the measurement volume. A light arm was positioned at the exit of the laser to direct the laser through the Perspex section of the model, minimising reflections and allowing the capture of both the suction and pressure sides of the aerofoil if required. Insight V3V-4G software was used to coordinate the laser pulses and image capture at a repetition rate of 1kHz and laser pulse separation of 30 microseconds.

The pillar sensors are laser-cut sheets of silicone rubber which are cut into shape to fit the prototype model, and such that the pillars are emanating from the suction surface.

In order to characterise the response of the pillars and to draw accurate conclusions about the surrounding flow, it is important to understand the structural properties. The pillars emanate from a silicone sheet clamped between the sections of the wing, thus acting as a cantilevered beam of uniform cross-section. The cross section of the pillar was found under 200x microscope. This shows slight variations in the thickness over the length of the pillar. Due to the process of manufacturing, there are no visible variations in pillar width. Simulations were subsequently carried out to show the sensitivity of pillar tip deflection to these variations in loading.

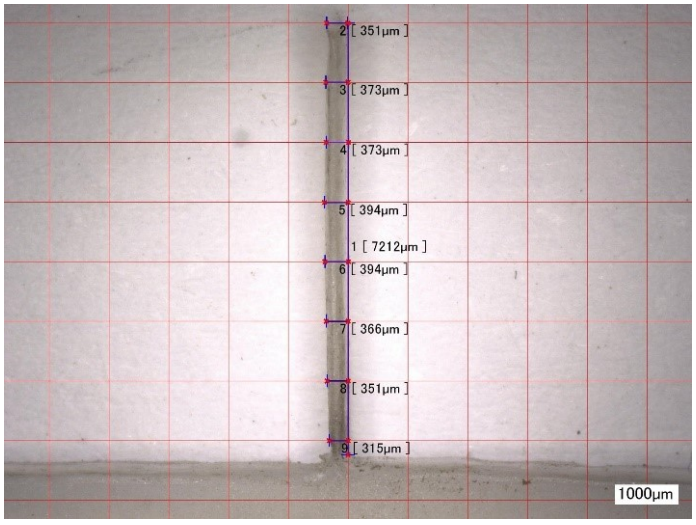

Figure 3. An image of one of the pillar sensors under a 200x microscope lens showing the details of the structure and pertinent dimensions

3. Results and Discussion

The pillars were tested in a specially built calibration tunnel, which produces a known jet of air to which the pillars were subjected (Fig. 5). From this, the pillar response in tip deflection to a known velocity, and thus a known load, was found.

The purpose of the FEA simulation is to use iterative methods of varying the material properties of a beam, of the same dimensions, that responds similarly to the pillar sensors over their operating and calibrated range. Given that the load and tip deflection are known experimentally from the calibration testing, and given the pillar dimensions are known to a good level of accuracy (Fig. 3), it is possible therefore to obtain from the FEA an accurate estimate of those material properties.

The forces acting on each pillar were obtained from the known velocity such that the drag coefficient was obtained from empirical data of flow over cylinders for Reynolds numbers $10^1 < Re < 10^3$ (Oertel, 2004). It was found with a power fit of an $R^2 = 0.967$, that:

$$C_d = 3.0244 \times Re^{-0.155} \tag{1}$$

The in-situ calibration is carried out on the first two pillars which experience clean oncoming flow. The flow visualisation over the first pillar from the calibration runs showed that the velocity experienced over the length of the pillar is very close to uniform, and thus the load can be approximated as a constant force over the length of the pillar.

$$F_d = \int q_\infty(l) \times b \times C_d(Re)\, dl \tag{2}$$

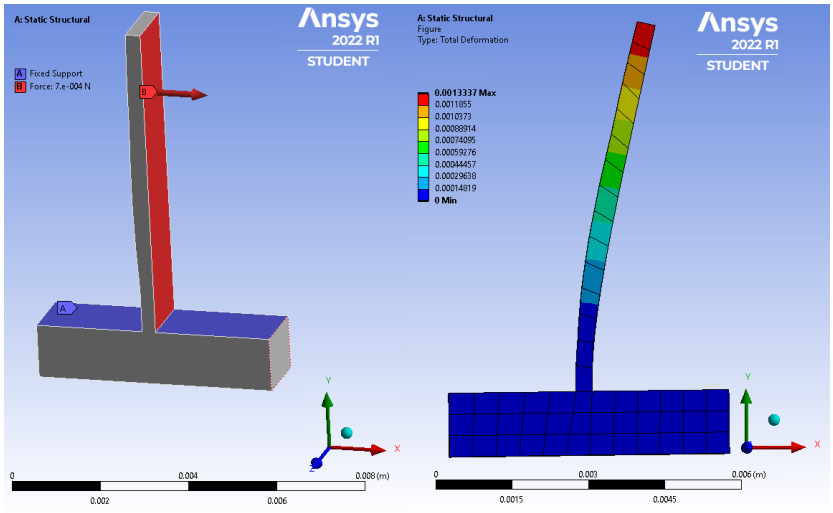

Figure 4. Setup and sample deformed result from FEA analysis

The FEA setup was then subjected to a range of loads that correspond to the loads experienced during the calibration testing of the pillars, and the material properties varied iteratively to obtain a simulation model which can be used to correlate the tip deflection to total applied loading of the first pillar. It was found that a Young's modulus of elasticity $E = 2.625MPa$ responded with values very close to the experimental values. The results were compared and are shown in (Fig.4).

The calibration wind tunnel is part of a project at City aimed at developing a small-scale wind tunnel that produces repeatable and predictable wall flows for the purpose of visualising the smaller scales over pillar sensors or similar apparatus while in-situ in order to develop a streamlined calibration process. This experimental rig is shown below.

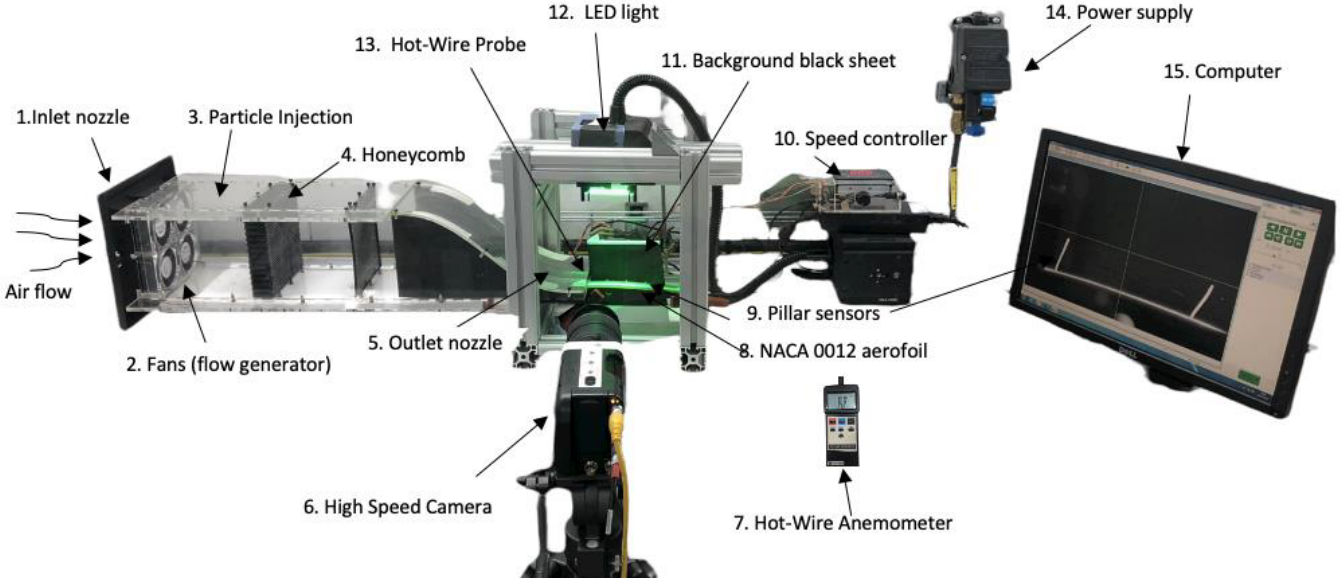

Figure 5. Experimental setup of the calibration tunnel, showing different components for various calibration related tests.

The pillar tips were marked and monitored using a high-speed camera. The tunnel with the current setup is able to produce stable flows up to approximately 10 m/s. Measurements were taken of the pillar deflections at various velocities between 2.5 m/s and 9.6 m/s to produce a calibration curve (Fig. 6) correlating the deflection of the first two pillars in mm with the free stream velocity experienced by the first pillar.

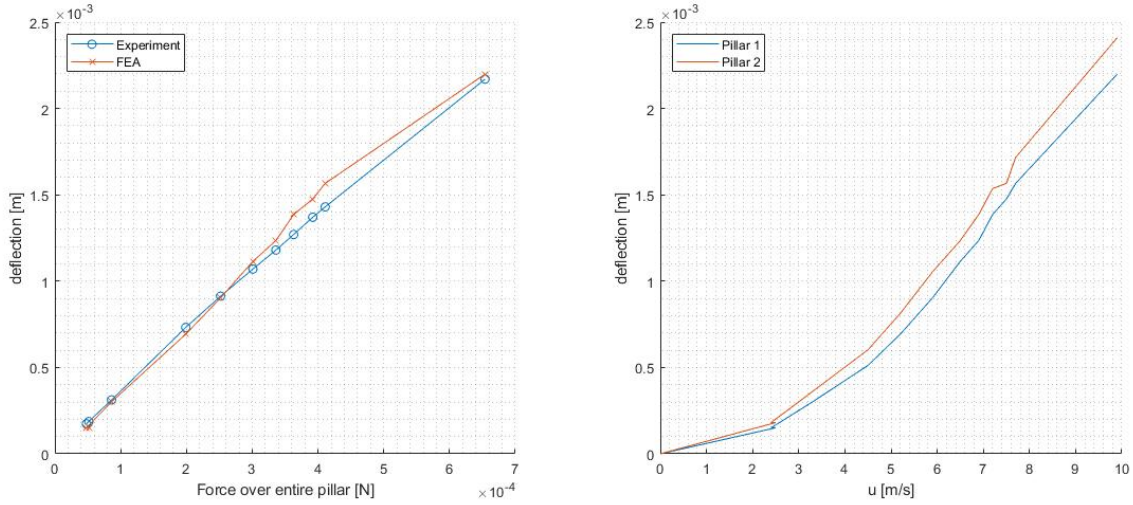

Figure 6. Left: The results from the FEA simulation are shown against those from the calibration experiment. Right: Deflection values from the results of the calibration tests.

The pillars both show a linear relationship of displacement with velocity for velocities above 4 m/s which corresponds to a slope of approximately 0.3 mm/[m/s] (0.32 and 0.34 for pillars 1 and 2 respectively) and Y-intercept of approximately -0.95 mm (0.96 and 0.94 for pillars 1 and 2 respectively). A higher resolution of velocity is required at velocities below 4 m/s to ascertain the trend accurately, however with the provided data it shows the relationship not to be linear. For all the current experiments in air, the free stream velocity is above 4 m/s which allows the free stream velocity to be ascertained at low angles of attack based only on the deflection of the first two pillars. The limitation here is that the calibration tunnel produces a jet which, over the first pillar produces repeatable and relatively steady flows, however as the jet is flowing over the suction peak of the aerofoil, albeit symmetric and at 0 incidence, and flowing into ambient conditions, the flow dissipates at a rate that is different from how the flow acts in the fully scaled wind tunnel. Hence why this method can only produce reliable results over the first two pillars, which can then be used to ascertain the velocities from the full-scale wind-tunnel experiments. Additionally, the positioning of the jet in the calibration run is such that the velocity is known at the pillar position by use of a hotwire anemometer, which is placed just aft of the suction peak of the aerofoil where the flow would normally be accelerated. Therefore, the velocity corresponding to the first pillar deflection in (Fig. 5) would not be the free-stream velocity, but rather the accelerated velocity at 15% chord, which can then be related to the free-stream velocity from known theory. (Winslow et al., 2018)

(Dickinson, 2010) investigated the effect of boundary layer changes on the deflection of flexible pillar structures. What can be seen is that as the boundary layer grows, an area close to the root of the pillar is subjected to flows that are slower than the free stream (Fig. 15), and thus lead to a reduction in overall deflection relative to the tip deflection if the pillar is subjected to a uniform flow. Since the pillars are fixed at the base, and are acting as cantilevers, changes in the forces closest to the fixed end result in smaller changes to the displacement of the free end than those further away, as they result in a smaller moment about the base. Thus, changes in the boundary layer must be large to result in a remarkable change in the tip deflection. This can be seen in the measurements by observing the total tip deflection of the pillars along the chord (Fig. 8). As the boundary layer grows, the pillar tip deflection can be seen to reduce. Tracking the amount of reduction in tip deflection of the pillars can give indication to the boundary layer's growth rate which is correlated with the angle of attack for a known Re.

The wind tunnel experiments were carried out in City's T2 wind tunnel. This is a closed-loop wind tunnel with a turbulence intensity of 0.8%. The test section is 0.81m x 1.22m where the model is mounted such that one end of the aerofoil spans to the floor while the free end is fitted with an end plate to negate tip effects. The model is a constant NACA0012 aerofoil of chord length 0.19m and span of 0.70m It consists of two sections clamped together with a transparent Perspex section between. This is such that a light sheet can pass through to allow simultaneous recording of pressure and suction side flows. The pillars are placed between the Perspex section and the aerofoil such that they emanate from the suction side. A series of experiments were carried out in this configuration at varying angles of attack and at a Reynolds number of 200,000, recording the pillar tip motion at a sampling rate of 500 Hz. These experiments produced results from which conclusions can be drawn about a variety of flow conditions.

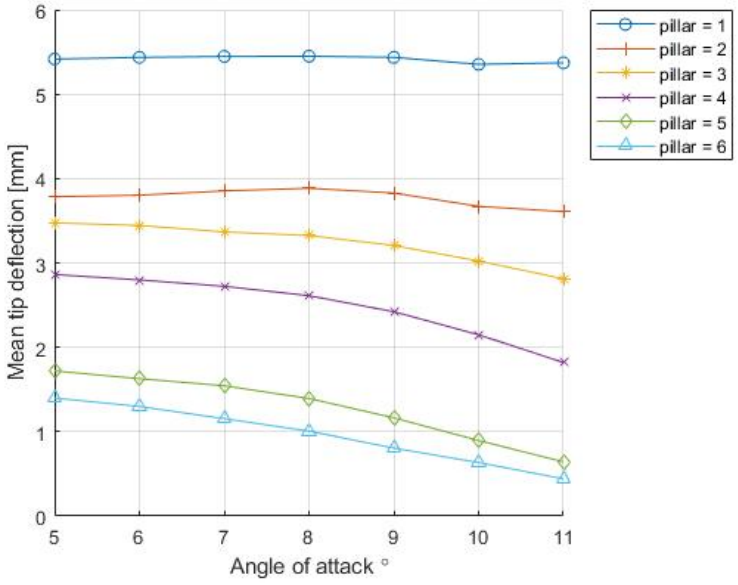

Figure 7. The mean tip deflection of the first two pillars were least affected by increase in angle of attack

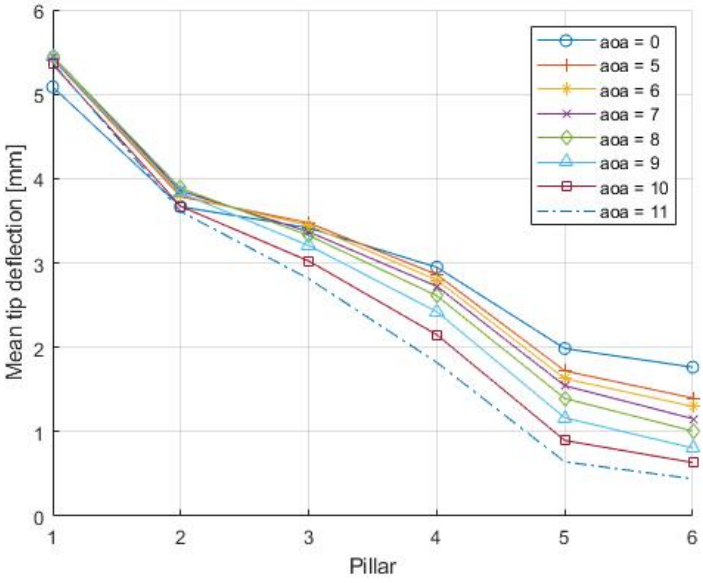

Figure 8. The mean tip deflection alone can give indication to flow conditions such at free-stream velocity and angle of attack

Firstly, by correlating the deflection of the first pillar with the calibration carried out, for low angles of attack, the free stream velocity can be found. This is because the mean deflection of the first two pillars are almost unaffected by changes of angle of attack until separation. This can be seen on the first datapoints of (Fig. 8) and is illustrated more clearly in (Fig. 7).

Additionally, as the angle of attack changes so does the boundary layer growth, which has an effect on the mean (time-averaged) bending of the pillars. Therefore, it can be seen from both (Fig. 1) and (Fig. 7) that the relative tip deflection of each pillar to the first pillar (or to the previous pillar) is smaller for higher angles of attack. This allowed for a measure of angle of attack simply from knowing the total deflection of the first pillar and the relative deflection of each other pillar, thus by knowing the gradient of the mean pillar deflection and the total deflection of the first pillar, the angle of attack can be known as there exists a unique combination of total and relative (time-averaged) tip deflection for each angle of attack. Additionally, it can be seen in (Fig. 9) that the amplitude of deflections is larger as the pillars move aft, and that at moderate angles of attack the aftmost pillars begin to reach negative deflections, which occur more frequently and to larger negative values at angles of attack immediate to stall.

The high flexibility of the pillars allowed also to give higher temporal resolution data which is useful for drawing conclusions on more intricate flow structures and to be used for characterising flow conditions. From the pillar deflection data, the frequency of oscillation can be found, which correlates with the frequency of flow structures over the aerofoil. These result from structures shedding off the laminar separation bubble during its breathing and shedding modes, thus allowing the timely identification of these flow phenomena unique to incipient separation.

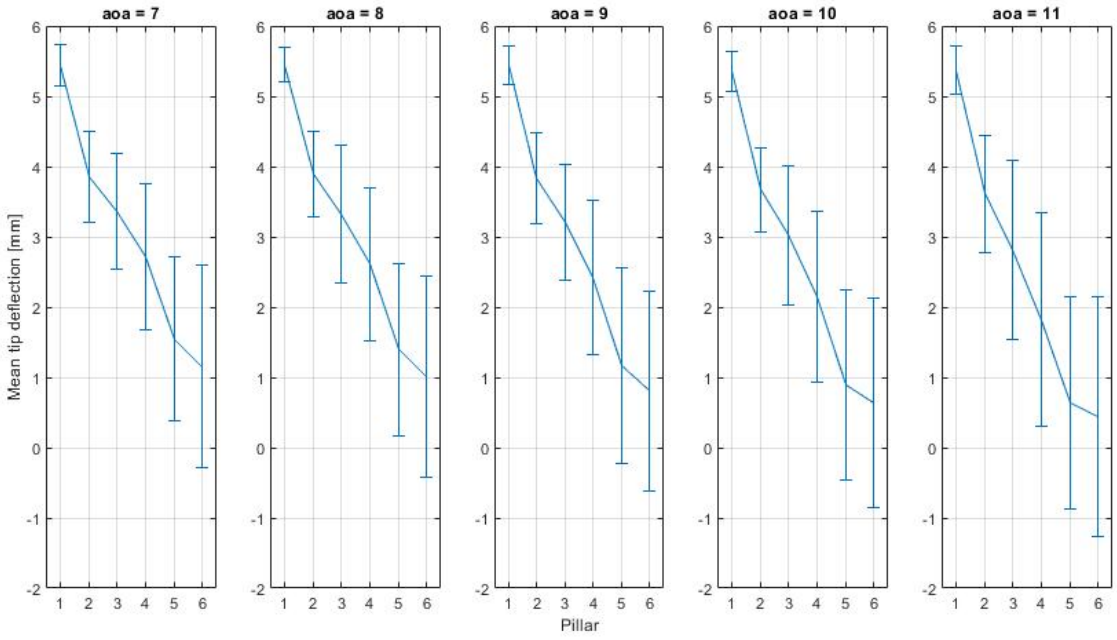

Figure 9. The amplitude of deflection for each pillar is shown for moderate, pre-stall angles of attack. The frequency and strength of negative (reversed) deflections can indicate proximity to separation and stall

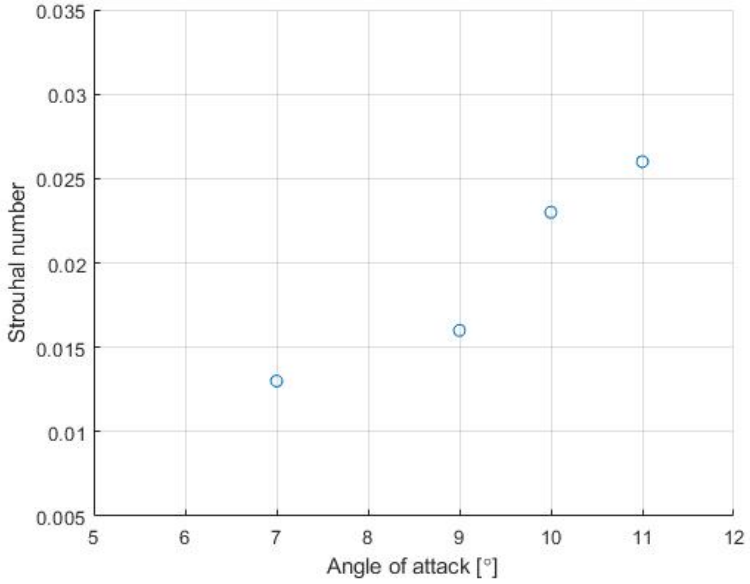

Figure 10. The Strouhal number of the detected oscillations is shown for pre-stall angles of attack.

(Fig. 14) shows the result from spectral analysis on the displacement values from a pillar at 45% chord. This is after applying a low-pass filter with a cutoff of 20 Hz to emphasise the low-frequency oscillations about which the study is concerned. The results for an angle of incidence of 0° are included. These show no discernible peaks of notable strength. At 7° a weak peak begins to form. What is noticed is that not only does the peak frequency increase with increase in angle of attack

but also the peak becomes stronger and more pronounced as the wing approaches stall. These are both quantities which can act as markers for instantaneous angle of attack sensing and indicators for incipient separation and stall. These peak frequencies correspond to Strouhal numbers shown in (Fig. 10).

To investigate the pillar tip deflection patterns leading up to stall, a ramp-up test was carried out where the pillar tip positions were tracked while the angle of incidence of the model was steadily changed from 0 to 15 degrees at a rate of (1.85 degrees/second) and a chord Reynolds number of 200k corresponding to a reduced frequency k (defined as (ρ.f.c)/U) of 0.5 x10-3. (Fig. 11) shows the results after applying filtering and correction where each pillar deflection position is plot against time. As the aerofoil approaches separation (approx. 5-6 s or 9-11 degrees) these low frequency oscillations become pronounced. This allows a clear distinction of specific oscillations unique to incipient separation.

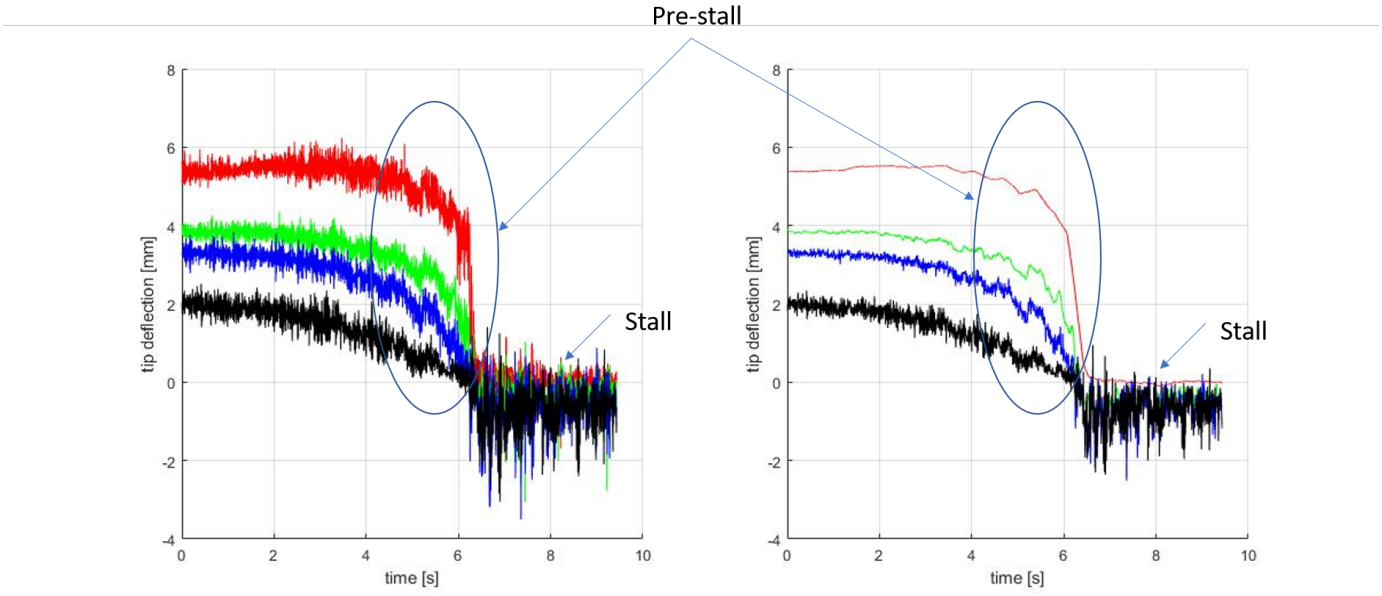

Figure 11. Results from ramp-up study showing oscillation and pre-stall behaviour of pillar tip deflections. The low frequency oscillations appear at pre-stall angles and are more apparent after smoothing (Right). Pillars 1 to 4 shown in red, green, blue and black respectively.

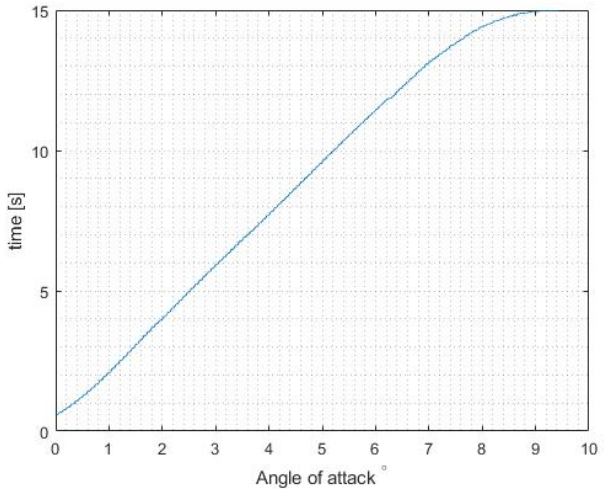

Figure 12. The incidence of the model from the ramp-up study was ramped up steadily from 0 degrees to 15 degrees in approximately 9 seconds

To validate the output from the tracking camera and compare both the tracking camera results and the recorded results to flow phenomena, a virtual probe reading was taken from the PIV results. (Fig. 13) shows the smoothed and filtered results from the third pillar from both the high-speed recordings and the tracking camera recordings, compared to the probe in the PIV results from the same position.

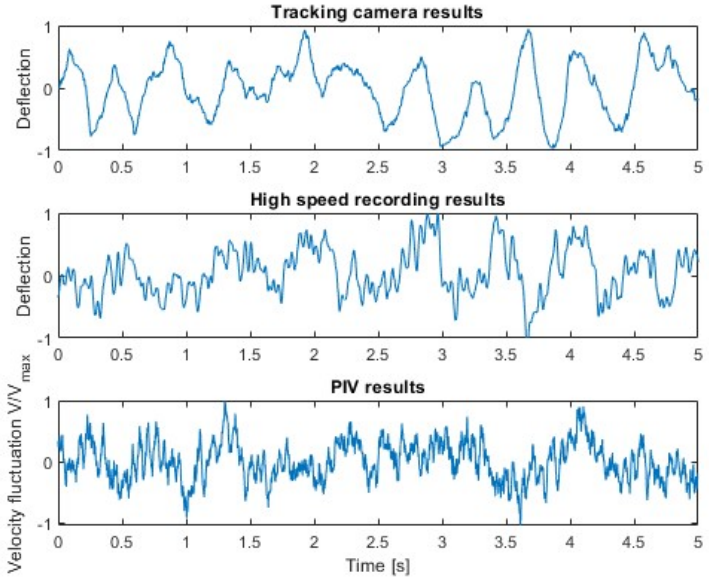

Figure 13. The normalised fluctuation component of deflection relative to the mean from the pillar placed at 45% chord are shown from 3 separate experiments, (a) taken from the tracking camera results, and in (b) from the processed images of the high-speed recording, compared here to (c) velocity fluctuations from the time-resolved PIV recordings, all at an incidence of 10 degrees.

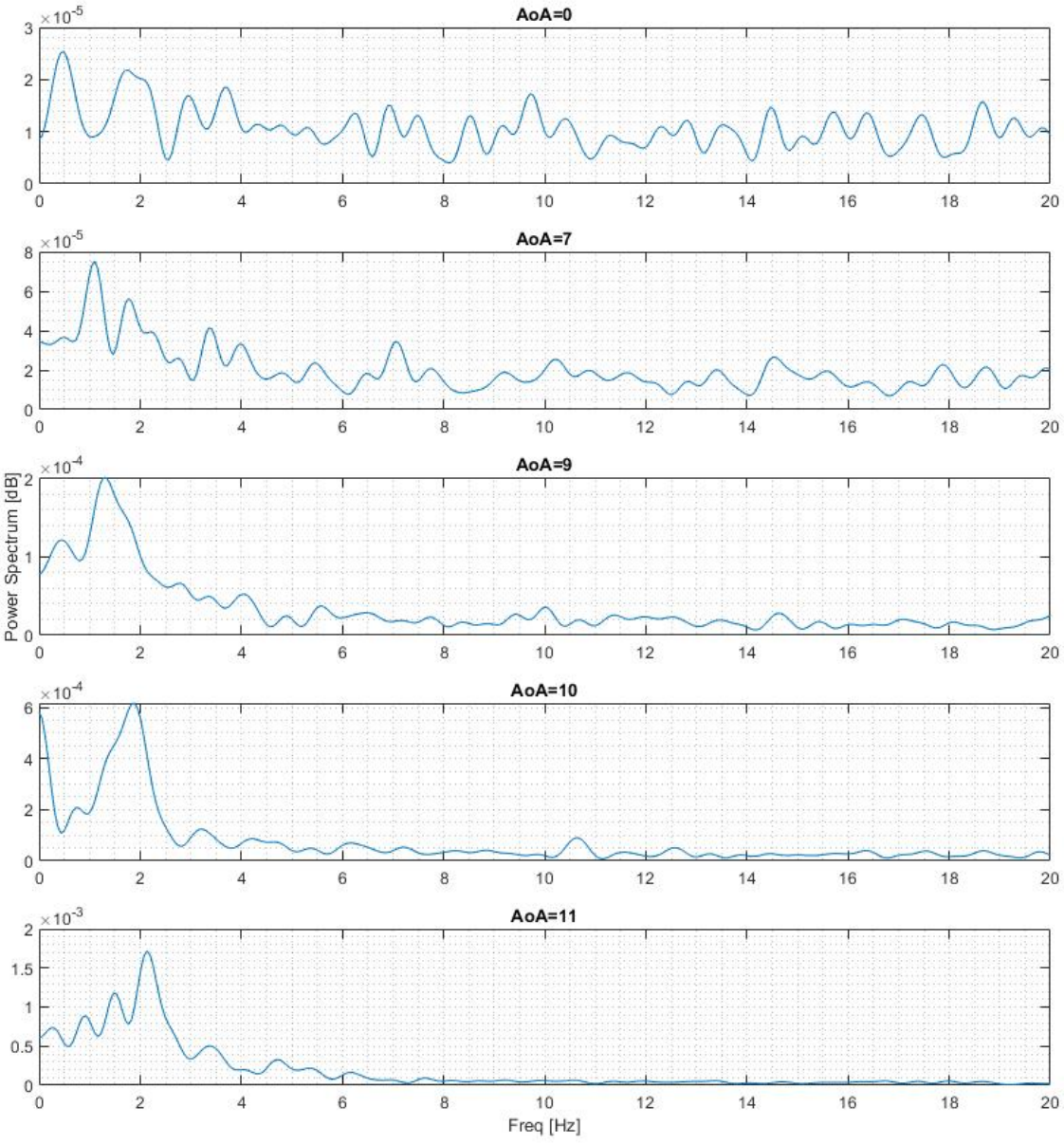

Figure 14. FFT of pillar deflections at increasing angles of attack showing the increase in frequency of the oscillations as stall is approached

4. Conclusions

This paper presents a series of results from experimental work on a NACA0012 aerofoil model using a system of flexible pillar sensors that emanate from the suction side of the aerofoil and are tracked optically acting as 'digital tufts'. These are monitored optically to give real-time high temporal resolution data that translates to flow velocities from which frequencies of flow structures over the wing can be analysed. These data are used to identify patterns that give rise to flow separation and stall.

From the results of the wind-tunnel testing of the sensors multiple simultaneous conclusions can be drawn. Firstly, simply from observing the time-averaged deflection of each pillar across the chord of the wing in the static wind-tunnel tests it was found that there exists a unique combination of total deflection for every angle of attack up to stall. That is, by simply observing the relative deflection of the sensors (which is represented by the gradient of the relative pillar deflections) the angle of attack is known due to the effect of changing boundary layer growth rate with angle of attack. As the boundary layer grows locally at each pillar, more of the pillar becomes immersed in slower BL flow which reduces the tip deflection as the overall force is reduced. Furthermore, instances of negative pillar deflection can be seen to be a marker of moderate angles of attack, the strength and frequency of which scale with angle of attack, and can be used as a pre-stall indicator.

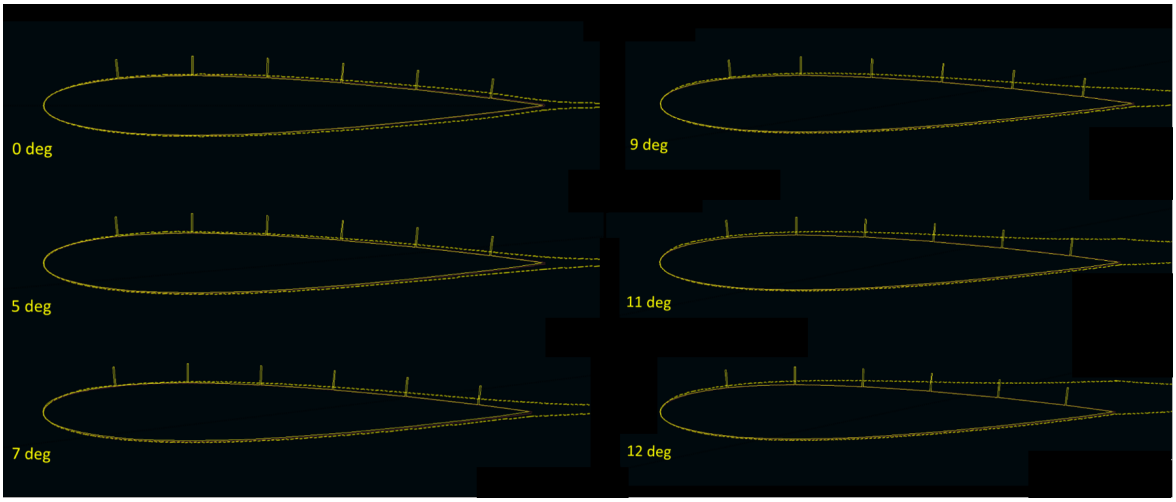

Figure 15. An xfoil estimation of the displacement thickness as the angle of attack approaches stall, with reference to pillar position and length

(Dickinson, 2010) characterised the sensitivity of similar hair-like structures to changes in BL thickness. This study has shown that these pillar sensor deflections are also affected by changes in boundary layer thickness. Thus, not only is it possible to draw from the relative tip deflections conclusions of angle-of-attack, which are most pertinent to this study concerned with application of these type-sensors on small-scale aviation, but also conclusions could be drawn about local boundary layer thickness and behaviour over an aerodynamic system for in-situ diagnostics and performance enhancement for a variety of systems such as wind-energy, high-performance motor-

ing (such as Formula 1 racing) aerodynamic monitoring and other aerodynamic or hydrodynamic flow optimization problems.

Moreover, the scale and high flexibility of the sensors allows the ability to monitor more subtle changes in velocity of various frequency ranges within the domain over the wing or aerodynamic structure. These can be correlated with known phenomena that are either found to be unique to a specific flight condition in testing, or learnt from application to be identified by training a specialised neural network. In this study, low-frequency oscillations were detected by the pillar sensors. These oscillations are hypothesised as flow-structures shedding from the breathing of a laminar separation bubble formed over the suction side of the wing. These structures shed with the breathing of this bubble and the frequency, as tracked by their effect on the flexible pillar sensors, can be correlated with the flight condition, specifically the angle of attack.

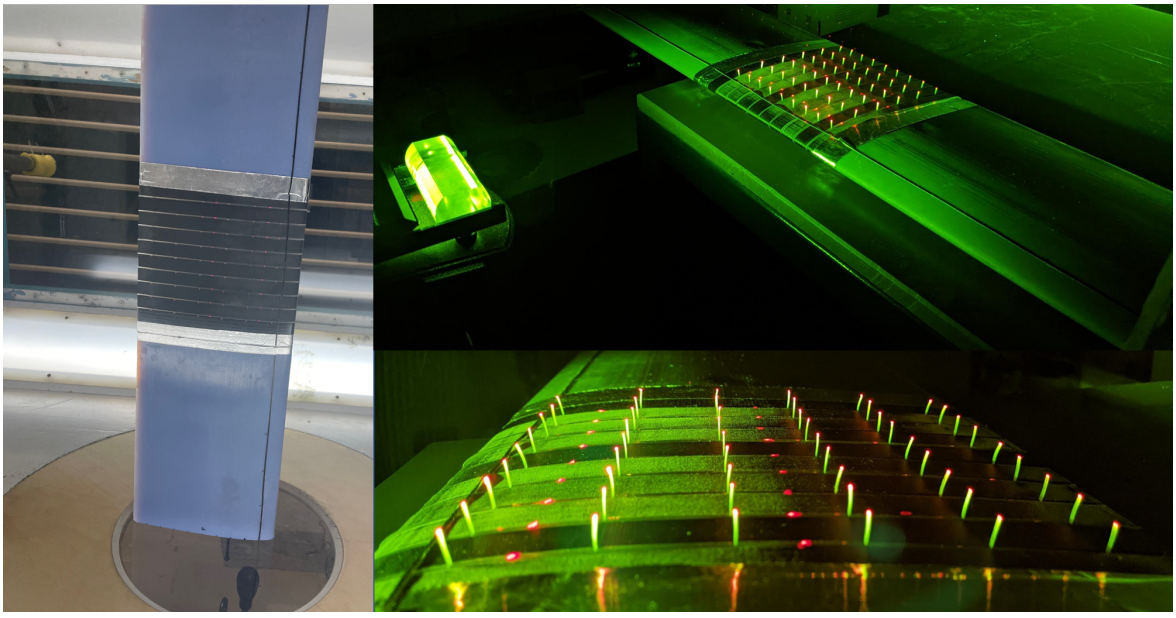

Figure 16. Setup of experiment with array of sensors attached. The tips are illuminated with green LED light

The pillar sensors can provide a multitude of velocity and velocity-derived data to be used for real-time diagnostics. Spectral analyses in conjunction with pattern recognition algorithms were used here to identify specific quantities unique to the flight conditions. However, introducing and training a specialised neural network to identify the local flow conditions, such as was carried out with similar nature-inspired sensors in (Elshalakani et al., 2020) is planned as further development of this system. Furthermore, spatial near-wall flow field recovery techniques can be applied from the relative sparse sensor placement using deep-learning. For timely decision making and response of the signals in an aeronautical system in-situ, the signals must be collected and processed 'on the fly' with optical systems that can filter out irrelevant data using physical means such as wavelength separation, in addition to computational means, and then process that data within the required time period. Using the on-line tracking (ProcImage 500-Eagle high-speed camera) during this study, it was possible to train the camera on the relevant pillar tips to instantaneously output a

time-series of coordinates corresponding to the pillar tip deflections for a specified time period and sampling rate. These type of recordings with multiple levels of filtering and pre-processing often are affected by corrupt or sparse data. Emerging technologies in reconstructing such data structures such as sparse representation and compressive sensing can allow for the timely and efficient onboard processing of these data for subsequent flight or flow control decision making (Callaham et al., 2019).

Spanwise data can be obtained by including an array of these pillar sensors over a wing. These can be used as "digital-tufts" over the skin of a wing in a wind-tunnel, or fitted onto the system in operation. Current work on the sensors is looking at local flow conditions at post-stall angles of attack as a way of characterising spanwise local stall phenomena simply from tip-deflection data of the pillars (Fig. 16). This, coupled with the developed signal processing from the sensors will allow the ability to provide diagnostic data for an aerodynamic system's performance over a wide regime of flow conditions.

Acknowledgements

The authors would like acknowledge and express their gratitude to the George Daniels Educational Trust, as well as BAE Systems and the Royal Academy of Engineering (grant RCSRF1617/4/11) for supporting their positions, and the Deutsche Forschungsgemeinschaft (DFG) for their support with provision of some of the optical systems used in this study. Additionally, the authors would like to acknowledge and express thanks to Alecsandra Court for her role in the continuation and development of the pillar sensor arrays and Ibrahim Kejje for his diligent work on the development of the calibration wind tunnel.

References

Brücker, C., Schlegel, D., & Triep, M. (2016). Feather vibration as a stimulus for sensing incipient separation in falcon diving flight. *Natural Resources*, *07*, 411–422.

Callaham, J. L., Maeda, K., & Brunton, S. L. (2019). Robust flow reconstruction from limited measurements via sparse representation. *Physical Review Fluids*, *4*(10), 103907.

Dickinson, B. T. (2010). Hair receptor sensitivity to changes in laminar boundary layer shape. *Bioinspiration & biomimetics*, *5*(1), 016002.

ElAwad, Y. A., & ElJack, E. M. (2019). Numerical investigation of the low-frequency flow oscillation over a naca-0012 aerofoil at the inception of stall. *International Journal of Micro Air Vehicles*, *11*, 1756829319833687.

Elshalakani, M., Muthuramalingam, M., & Bruecker, C. (2020). A deep-learning model for underwater position sensing of a wake's source using artificial seal whiskers. *Sensors*, *20*(12), 3522.

Li, Q., Stavropoulos-Vasilakis, E., Koukouvinis, P., Gavaises, M., & Bruecker, C. H. (2021). Micro-pillar sensor based wall-shear mapping in pulsating flows: In-situ calibration and measurements in an aortic heart-valve tester. *Journal of Fluids and Structures*, *105*, 103346.

Mohamed, A., Watkins, S., Clothier, R., Abdulrahim, M., Massey, K., & Sabatini, R. (2014). Fixed-wing mav attitude stability in atmospheric turbulence—part 2: Investigating biologically-inspired sensors. *Progress in Aerospace Sciences*, *71*, 1–13.

Oertel, H. (2004). *Prandtl's essentials of fluid mechanics*. Springer.

Selim, O., Gowree, E. R., Lagemann, C., Talboys, E., Jagadeesh, C., & Brücker, C. (2021). Peregrine falcon's dive: Pullout maneuver and flight control through wing morphing. *AIAA Journal*, *59*(10), 3979–3987.

Soulier, A., Braud, C., Voisin, D., & Podvin, B. (2021). Low-reynolds-number investigations on the ability of the strip of e-telltale sensor to detect the flow features over wind turbine blade section: flow stall and reattachment dynamics. *Wind Energy Science*, *6*(2), 409–426.

Tanaka, H. (2004). Flow visualization and piv measurements of laminar separation bubble oscillating at low frequency on an airfoil near stall. In *24th international congress of the aeronautical sciences* (pp. 1–15).

Winslow, J., Otsuka, H., Govindarajan, B., & Chopra, I. (2018). Basic understanding of airfoil characteristics at low reynolds numbers (10 4–10 5). *Journal of Aircraft*, *55*(3), 1050–1061.